

Learning Generalized Hypergeometric Distribution (GHD) DAG models

Gunwoong Park¹

¹ Department of Statistics, University of Seoul

Abstract

In this paper, we introduce a new class of identifiable DAG models, where each node has a conditional distribution given its parents belongs to a family of generalized hypergeometric distributions (GHD). a family of generalized hypergeometric distributions (GHD) includes a lot of discrete distributions such as Binomial, Beta-binomial, Poisson, Poisson type, displaced Poisson, hyper-Poisson, logarithmic, and many more. We prove that if the data drawn from the new class of DAG models, one can fully identify the graph. We further provide a reliable and tractable algorithm that recovers the directed graph from finitely many data. We show through theoretical results and simulations that our algorithm is statistically consistent even in high-dimensional settings ($n > p$) if the degree of the graph is bounded, and performs well compared to state-of-the-art DAG-learning algorithms.

1 Introduction

Probabilistic directed acyclic graphical (DAG) models or Bayesian networks provide a widely used framework for representing causal or directional dependence relationships among many variables. One of the fundamental problems associated with DAG models or Bayesian networks is causal structure learning given a sample from the joint distribution $P(G)$.

Prior work has addressed the question of identifiability for different classes of joint distribution $P(G)$ over a set of vertices of a graph. [4, 5] show the Markov equivalence class (MEC) where graphs that belong to the same MEC have the same (conditional) independence structure, the same undirected edges and the same unshielded colliders. In addition, a graph structure can be recovered up to MEC from any $P(G)$ under the faithfulness condition or some milder conditions.

Recently, many works show fully identifiable DAG models under stronger assumptions on $P(G)$. [13] proves that Gaussian structural equation models with equal or known error variances are identifiable. In addition, [15] show that linear non-Gaussian models where each variable is determined by a linear function of its parents plus a non-Gaussian error term are identifiable. [6, 10, 14] relax the assumption of linearity and prove that nonlinear additive noise models where each variable is determined by a non-linear function of its parents plus an error term are identifiable under suitable regularity conditions. Instead of considering linear or additive noise models, [11, 12] introduce discrete DAG models where each conditional node distribution given its parents belongs to the exponential family of discrete distributions such as Poisson, binomial, and negative binomial. They prove that the discrete DAG models are identifiable as long as the variance is a *quadratic* function of the mean.

In this paper, we generalize the main idea in [11, 12] to a *family of generalized hypergeometric distributions (GHD)* that includes Poisson, Poisson type, displaced Poisson, Hyper Poisson, binomial, negative binomial, beta-binomial, logarithmic, and many more (see more examples in Table 1 and ([7, 2, 8])). We introduce a new class of identifiable DAG models where each conditional node distribution given its parents belongs to a family of GHDs. We prove that generalized hypergeometric distribution (GHD) DAG models are identifiable using a *convex* relationship between the mean and the r -th factorial moment for some positive integer $r = 2, 3, \dots$

We also develop the reliable and scalable Moments Ratio Scoring (MRS) algorithm which learns any large-scale GHD DAG model. We provide statistical guarantees for recovering a graph to show that our MRS algorithm is consistent for learning GHD DAG models, even in the high-dimensional $p > n$ setting when the degree of the graph is bounded. We demonstrate through simulations that our MRS algorithm performs better than state-of-the-art algorithms in terms of recovering a graph structure.

The remainder of this paper is structured as follows: Section 2.1 summaries the necessary notation, Section 2.2 defines GHD DAG models and Section 2.3 proves that GHD DAG models are identifiable. In Section 3, we derive the moment ratio scoring (MRS) function for model selection and develop a polynomial-time algorithm for learning GHD DAG models. Section 3.1 provides its theoretical guarantees provided that the degree of the graph d is bounded, Section 3.2 provides its computational complexity. Section 4 empirically evaluates our methods compared to state-of-the-art DAG learning algorithms.

2 GHD DAG Models and Identifiability

In this section, we first introduce some necessary notations and definitions for directed acyclic graph (DAG) models. Then we propose of our novel generalized hypergeometric distribution (GHD) DAG models. Then we discuss its identifiability using a convex relationship between the mean and r -th moment for some positive integer $r = 2, 3, \dots$

2.1 Set-up and notation

A DAG $G = (V, E)$ consists of a set of nodes $V = \{1, 2, \dots, p\}$ and a set of directed edges $E \in V \times V$ with no directed cycles. A directed edge from node j to k is denoted by (j, k) or $j \rightarrow k$. The set of *parents* of node k denoted by $\text{Pa}(k)$ consists of all nodes j such that $(j, k) \in E$. If there is a directed path $j \rightarrow \dots \rightarrow k$, then k is called a *descendant* of j and j is an *ancestor* of k . The set $\text{De}(k)$ denotes the set of all descendants of node k . The *non-descendants* of node k are $\text{Nd}(k) := V \setminus (\{k\} \cup \text{De}(k))$. An important property of DAGs is that there exists a (possibly non-unique) *ordering* $\pi = (\pi_1, \dots, \pi_p)$ of a directed graph that represents directions of edges such that for every directed edge $(j, k) \in E$, j comes before k in the causal ordering. Hence learning graph is equivalent to learning an ordering with known undirected edges without directions.

We consider a set of random variables $X := (X_j)_{j \in V}$ with probability distribution $P(X_j)$ taking values in probability space \mathcal{X}_v over the nodes in G . Suppose that a random vector X has joint probability density function $P(G) = P(X_1, X_2, \dots, X_p)$. For any subset S of V , let $X_S := \{X_j : j \in S \subset V\}$ and $\mathcal{X}(S) := \times_{j \in S} \mathcal{X}_j$. For $j \in V$, $P(X_j | X_S)$ denotes the conditional distribution of a random variable X_j given a random vector X_S . Then, a probabilistic DAG model has the following factorization [9]:

$$P(G) = P(X_1, X_2, \dots, X_p) = \prod_{j=1}^p P(X_j | X_{\text{Pa}(j)}), \quad (1)$$

where $P(X_j | X_{\text{Pa}(j)})$ is the conditional distribution of X_j given its parents $X_{\text{Pa}(j)} := \{X_k : k \in \text{Pa}(j)\}$.

We suppose that the data consist of n i.i.d observations $X^{1:n} := (X^{(i)})_{i=1}^n$ where $X^{(i)} := (X_1^{(i)}, X_2^{(i)}, \dots, X_p^{(i)})$ is a p -variate random vector. We use the notation $\hat{\cdot}$ to denote an estimate based on $X^{1:n}$.

2.2 Generalized Hypergeometric Distribution (GHD) DAG Models

In this section, we begin by introducing a family of generalized hypergeometric distributions (GHDs) defined by [7]. A family of GHDs includes a large number of discrete probability laws and have probability generating functions that may be expressed in terms of the generalized hypergeometric series. We borrow the notations and terminology in [8] to explain detailed properties of a family of GHDs. Let $(a)^j = a(a+1) \cdots (a+j-1)$ and $(a)^0 = 1$. In addition, generalized hypergeometric function is:

$${}_pF_q[a_1, \dots, a_p; b_1, \dots, b_q; \theta] := \sum_{j \geq 0} \frac{(a_1)^j \cdots (a_p)^j \theta^j}{(b_1)^j \cdots (b_q)^j j!}.$$

GHDs are known to have probability generating functions of the form.

$$G(s) = \frac{{}_pF_q[a_1, \dots, a_p; b_1, \dots, b_q; \theta s]}{{}_pF_q[a_1, \dots, a_p; b_1, \dots, b_q; \theta]} = {}_pF_q[a_1, \dots, a_p; b_1, \dots, b_q; \theta(s-1)] \quad (2)$$

This class of distributions includes the Binomial, Beta-binomial distribution, Poisson, Poisson type, displaced Poisson, hyper-Poisson, logarithmic, generalized log-series and many other distributions. We provide more examples with their probability generating functions in Table 1.

Now we define the generalized hypergeometric distribution (GHD) DAG models.

Definition 2.1 (GHD DAG Models). The DAG models belongs to generalized hypergeometric distribution (GHD DAG) models if each conditional distribution given its parents belongs to a family of generalized hypergeometric distributions and the parameter depend only on its parents.

A good example of GHD DAG models is a Poisson DAG model in [11] where a conditional distribution of each node $j \in V$ given its parents is Poisson and the rate parameter is $g_j(\text{Pa}(j))$. In addition, the exponential family of discrete distributions discussed in [12] is also subset of a family of GHDs. Hence, our class of DAG models is strictly broader the previously studied identifiable discrete DAG models.

Distributions	p.g.f. $G(s)$	Parameters
Poisson	${}_0F_0[; ; \lambda(s-1)]$	$\lambda > 0$
Hyper-Poisson (Bardwell and Crow)	${}_1F_1[1; b; \lambda(s-1)]$	$\lambda > 0$
Negative Binomial	${}_1F_0[k; ; p(s-1)]$	$k, p > 0$
Poisson Beta	${}_1F_1[a; a+b; \lambda(s-1)]$	$a, b, \lambda > 0$
Negative Binomial Beta	${}_2F_1[k, a; a+b; \lambda(s-1)]$	$k, a, b, \lambda > 0$
STERRED Geometric	${}_2F_1[1, 1; 2; q(s-1)/(1-q)]$	$1 > q > 0$
Shifted UNSTERRED Poisson	${}_1F_1[2; 1; \lambda(s-1)]$	$1 \geq \lambda > 0$
Shifted UNSTERRED Negative Binomial	${}_2F_1[k, 2; 1; p(s-1)]$	$p > 0, (p+1)/p \geq k > 0$

Table 1: Examples of Hypergeometric Distribution and their probability generating functions $G(s)$

GHD DAG models have some useful properties for recovering graph structure. The first property is the recurrence relation involving factorial moments.

Proposition 2.2 (Constant Moments Ratio (CMR) property). *Suppose that a conditional distribution of X_j given its parents belongs to hypergeometric family of discrete probability distributions and its probability generating functions has the form in Eqn.(2). For any $j \in V$ and any integer $r = 2, 3, \dots$, there exists a r -th factorial constant moments ratio (CMR) function $f_j^{(r)}(x) = x^r \prod_{i=1}^p \left(\frac{(a_i+r-1)_r}{a_i^r} \right) \prod_{k=1}^q \left(\frac{b_k^r}{(b_k+r-1)_r} \right)$ such that*

$$\mathbb{E} \left((X_j)_r \mid X_{Pa(j)} \right) = \mathbb{E} \left(X_j(X_j-1) \cdots (X_j-r+1) \mid X_{Pa(j)} \right) = f_j^{(r)} \left(\mathbb{E}(X_j \mid X_{Pa(j)}) \right).$$

where $(x)_r := x!/(x-r)!$.

The detail of the proof is provided in Appendix. This proposition claims that GHD DAG models have the r -th constant moments ratio (CMR) property that r -th factorial moment is a function of the expectation. We will exploit the CMR property for model identifiability in the next section.

2.3 Identifiability

In this section we prove that GHD DAG models are identifiable, which means one can infer the graph from the probability distribution $P(G)$. To provide intuition, we show identifiability for the bivariate Poisson DAG model in [11]. Consider all three models illustrated in Figure 1: $G_1 : X_1 \sim \text{Poisson}(\lambda_1), X_2 \sim \text{Poisson}(\lambda_2)$, where X_1 and X_2 are independent; $G_2 : X_1 \sim \text{Poisson}(\lambda_1)$ and $X_2 \mid X_1 \sim \text{Poisson}(g_2(X_1))$; and $G_3 : X_2 \sim \text{Poisson}(\lambda_2)$ and $X_1 \mid X_2 \sim \text{Poisson}(g_1(X_2))$ for arbitrary positive functions $g_1, g_2 : \mathbb{N} \cup \{0\} \rightarrow \mathbb{R}^+$. Our goal is to determine whether the underlying graph is G_1, G_2 or G_3 from $P(G)$.

We exploit the r -th constant moments ratio of Poisson distribution, $\mathbb{E}((X)_r) = \mathbb{E}(X)^r$ for any positive integer r . For G_1 , $\mathbb{E}((X_1)_r) = \mathbb{E}(X_1)^r$ and $\mathbb{E}((X_2)_r) = \mathbb{E}(X_2)^r$. For G_2 , $\mathbb{E}((X_1)_r) = \mathbb{E}(X_1)^r$, while

$$\mathbb{E}((X_2)_r) = \mathbb{E}(\mathbb{E}((X_2)_r \mid X_1)) = \mathbb{E}(\mathbb{E}(X_2 \mid X_1)^r) > \mathbb{E}(\mathbb{E}(X_2 \mid X_1))^r = \mathbb{E}(X_2)^r,$$

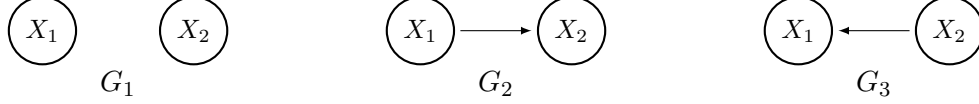


Figure 1: Bivariate directed acyclic graphs of G_1 , G_2 and G_3

as long as $r \geq 2$. The inequality follows from the Jensen's inequality.

Similarly for G_3 , $\mathbb{E}((X_2)_r) = \mathbb{E}(X_2)^r$ and $\mathbb{E}((X_2)_r) > \mathbb{E}(X_2)^r$ as long as $r \in \{2, 3, \dots\}$. Hence we can distinguish graphs G_1 , G_2 , and G_3 by testing whether the moments ratio $\mathbb{E}((X_j)_r)/\mathbb{E}(X_j)^r$ is greater than or equal to 1.

For the general case of GHD DAG models, the moments ratio may not be greater than one unless r -th factorial CMR function $f_j^{(r)}$ in Prop.2.2 is strictly convex. More precise identifiability condition is following.

Assumption 2.3 (Identifiability Condition). Consider the class of GHD DAG models with the r -th factorial CMR function $(f_j^{(r)})_{j \in V}$ in Prop. 2.2. For all $j \in V$, non-empty $\text{Pa}_0(j) \subset \text{Pa}(j)$, and $S_j \subset \text{Nd}(j) \setminus \text{Pa}_0(j)$,

$$\mathbb{E}((X_j)_r | X_{S_j}) > f_j^{(r)}(\mathbb{E}(X_j | X_{S_j})). \quad (3)$$

We recall the CMR property in Prop 2.2 that $\mathbb{E}((X_j)_r | X_{S_j}) = \mathbb{E}(f_j^{(r)}(\mathbb{E}(X_j | X_{\text{Pa}(j)})) | X_{S_j})$ for $S_j = \text{Pa}(j) \setminus \text{Pa}_0(j)$. Hence, the following two conditions are required to hold Assumption 2.3; (i) $f_j^{(r)}$ is strictly convex by Jensen's inequality; and (ii) the r -th factorial moment of each node should be influenced by all of its parents otherwise equality holds.

Now we state the first main result that general p -variate GHD DAG models are identifiable.

Theorem 2.4 (Identifiability). *Under Assumption 2.3, the class of GHD DAG models is identifiable.*

We defer the proof in Appendix. The key idea of the identifiability is to search the smallest conditioning set S_j for each node j such that a moments ratio $\mathbb{E}((X_j)_r | X_{S_j})/f_j^{(r)}(\mathbb{E}(X_j | X_{S_j})) = 1$. Theorem 2.4 claims that the assumption on node distributions is sufficient to uniquely identify GHD DAG models. In other words, the well-known assumptions such as faithfulness, non-linear causal relation, non-Gaussian additive noise assumptions are not necessary ([13, 15, 6, 10, 14]).

Theorem 2.4 implies that Poisson DAG models are identifiable because the r -th factorial CMR function $f_j^{(r)}(x) = x^r$ is strictly convex on the nonnegative support, and hence Assumption 2.3 is satisfied. In addition, Hyper-Poisson DAG models with arbitrary dispersion parameter b are identifiable because $f_j^{(r)}(x) = x^r \frac{2b^{r-1}}{(b+r)^r}$. We provide numerical experiments on Poisson and Hyper-Poisson DAG models to support our idea that GHD models are identifiable in Section 4.

3 Algorithm

In this section, we present our Moment Ratio Scoring (MRS) algorithm for learning GHD DAG models. Our MRS algorithm has two main steps: 1) identifying the skeleton (i.e., edges without their directions)

using existing skeleton learning algorithms; and 2) estimating the ordering of the DAG G using moment ratio scoring and assign the directions to the skeleton based on the estimated ordering.

Although GHD DAG models can be recovered only from the r -th CMR property according to Thm 2.4, our algorithm exploits the skeleton to reduce the search space of DAGs. From the idea of constraining the search, our algorithm achieves computational and statistical improvements. More precisely, Step 1) provides *candidate parents* set for each node. The concept of candidate parents set exploits two properties; (i) the neighborhood of a node j in the graph denoted by $\mathcal{N}(j) := \{k \in V \mid (j, k) \text{ or } (k, j) \in E\}$ is a superset of its parents, and (ii) a node should appear later than its parents in the ordering. Hence, the candidate parents set for a given node j is the intersection of its neighborhood and elements of the ordering which appear before that node j , and is denoted by $C_{mj} := \mathcal{N}(j) \cap \{\pi_1, \pi_2, \dots, \pi_{m-1}\}$ where m^{th} element of the ordering is j (i.e., $\pi_m = j$). The estimated candidate parents set is $\hat{C}_{mj} := \hat{\mathcal{N}}(j) \cap \{\hat{\pi}_1, \hat{\pi}_2, \dots, \hat{\pi}_{m-1}\}$ that is specified in Alg. 1

This candidate parents set is used as a conditioning set for a moments ratio score in Step 2). If the candidate parents set is not used, the size of the conditioning set for a ratio of moments score could be $p - 1$. Since Step 2) computes the r -th factorial moments, both the computation and sample complexities depend significantly on the number of variables we condition on as illustrated in Sections 3.1 and 3.2. Therefore by making the conditioning set for a moments ratio score of each node as small as possible, we gain computational and statistical improvements.

The idea of reducing the search space of DAGs have been studied in many sparse candidate algorithms. Hence for Step 1) of our algorithm, any off-the-shelf candidate parents set learning algorithms can be applied such as the MMPC [17] and SC algorithms [3]. Moreover, any standard MEC learning algorithms such as PC [16], GES [1] can be exploited because MEC provides the skeleton of a graph.

Step 2) of the MRS algorithm involves learning the ordering by comparing moment ratio scores of nodes using (4). The basic idea is to test which nodes have moment ratio score 1. The ordering is determined one node at a time by selecting the node with the smallest moment ratio score because the correct element of the ordering has a score 1, otherwise strictly greater than 1 in population.

Regarding the calculation of moments ratio scores, suppose that there are n i.i.d. samples $X^{1:n}$ drawn from GHD DAG models with a r -th factorial CMR function $f_j^{(r)}$. Instead of using the ratio $\mathbb{E}((X)_r)/f^{(r)}(\mathbb{E}(X))$, we use $\mathbb{E}(X^r)/(\mathbb{E}(X)^r - \sum_{k=0}^{r-1} s(r, k)\mathbb{E}(X^k))$ where $s(r, k)$ is Stirling numbers of the first kind. This alternative ratio score is from the fact that $(x)_r = \sum_{k=0}^r s(r, k)x^k$ and hence $\mathbb{E}(X^r) = f^{(r)}(\mathbb{E}(X)) - \sum_{k=0}^{r-1} s(r, k)\mathbb{E}(X^k)$. This alternative ratio score avoids the invalid scores due to the invalid r -th factorial moment when $X^{1:n} \leq r$. More precisely, the moment ratio score in Step 2) of Alg. 1 involves the following

equations:

$$\begin{aligned}\widehat{\mathcal{S}}_r(1, j) &:= \frac{\widehat{\mathbb{E}}(X_j^r)}{f_j(\widehat{\mathbb{E}}(X_j)) - \sum_{k=0}^{r-1} s(r, k) \widehat{\mathbb{E}}(X_j^k)}, \text{ and} \\ \widehat{\mathcal{S}}_r(m, j) &:= \sum_{x \in \mathcal{X}_{\widehat{C}_{mj}}} \frac{n_{\widehat{C}_{mj}}(x)}{n_{\widehat{C}_{mj}}} \left[\frac{\widehat{\mathbb{E}}(X_j^r | X_{\widehat{C}_{mj}} = x)}{f_j(\widehat{\mathbb{E}}(X_j | X_{\widehat{C}_{mj}} = x)) - \sum_{k=0}^{r-1} s(r, k) \widehat{\mathbb{E}}(X_j^k)} \right].\end{aligned}\quad (4)$$

where \widehat{C}_{mj} is the estimated candidate parents set of node j for the m^{th} element of the ordering. In addition, $n(x_S) := \sum_{i=1}^n \mathbf{1}(X_S^{(i)} = x_S) \mathbf{1}(n(x_S) \geq N_{\min})$ refers to the truncated conditional sample size for x_S , and $n_S := \sum_{x_S} n(x_S)$ refers to the total truncated conditional sample size for variables X_S . We discuss the choice of N_{\min} later in Sec 3.1. Lastly, we use the method of moments estimators $\frac{1}{n} \sum_{i=1}^n ((X_j^{(i)})^r)$ and $f_j(\frac{1}{n} \sum_{i=1}^n X_j^{(i)})$ as unbiased estimators for $\mathbb{E}(X_j^r)$ and $f_j(\mathbb{E}(X_j))$, respectively.

Since there are many conditional distributions, our moments ratio score is the weighted average of the r -th moments ratios of each distribution. As demonstrated in Sec 2.3, the correct elements of an ordering achieve the score one, otherwise greater than one in population. We only use the subset of samples that ensures we have enough samples for each element.

Finally, finding the set of parents of node j boils down to selecting the parents out of all elements before node j in the ordering. Hence given the estimated ordering from Step 2), estimating the graph is to assign the directions to the skeleton estimated by Step 1).

3.1 Statistical Guarantees

In this section, we provide theoretical guarantees for Step 2) of the MRS algorithm. We provide sample complexity for the MRS algorithm given that the undirected graph is correctly estimated in Step 1). The main result is expressed in terms of the triple; n sample size, p graph size, and d graph complexity.

We begin by discussing three required conditions that the MRS algorithm recovers a graph.

Assumption 3.1. Consider the class of GHD DAG models with r -th factorial CMR function $f_j^{(r)}$ specified in Prop. 2.2. For all $j \in V$ and any non-empty $\text{Pa}_0(j) \subset \text{Pa}(j)$ where $S_j \subset \text{Nd}(j) \setminus \text{Pa}_0(j)$,

- (a) there exists an $M_{\min} > 0$ such that

$$\mathbb{E}((X_j)_r | X_{S_j}) - f_j(\mathbb{E}(X_j | X_{S_j})) > M_{\min}.$$

- (b) there exists an V_1 such that

$$\mathbb{E}(\exp(X_j) | X_{\text{Pa}(j)}) < V_1.$$

- (c) there are some elements $x_{S_j} \in \mathcal{X}_{S_j}$ such that

$$\sum_{i=1}^n \mathbf{1}(X_{S_j}^{(i)} = x_{S_j}) \geq N_{\min}.$$

Algorithm 1: Moments Ratio Scoring (MRS)

Input : n i.i.d. samples from a GHD DAG model, $X^{1:n}$

Output: Estimated ordering $\hat{\pi}$ and an edge structure, $\hat{E} \in V \times V$

Step 1: Estimate the candidate parents set for each node;

Step 2: Estimate the causal ordering using r -th moments ratio scores;

for $j \in \{1, 2, \dots, p\}$ **do**

 | Calculate r -th moments ratio scores $\hat{\mathcal{S}}_r(1, j)$ using Eqn (4);

end

The first element of the causal ordering $\hat{\pi}_1 = \arg \min_m \hat{\mathcal{S}}_r(1, m)$;

for $m = \{2, \dots, p-1\}$ **do**

for $j \in \{1, 2, \dots, p\} \setminus \{\hat{\pi}_1, \dots, \hat{\pi}_{m-1}\}$ **do**

 | Find candidate parents set $\hat{C}_{m,j} = \hat{\mathcal{N}}(j) \cap \{\hat{\pi}_1, \dots, \hat{\pi}_{m-1}\}$;

 | Calculate r -th moments ratio scores $\hat{\mathcal{S}}_r(m, j)$ using Eqn (4);

end

 The m^{th} element of a causal ordering $\hat{\pi}_m = \arg \min_j \hat{\mathcal{S}}(m, j)$;

end

The last element of the ordering $\hat{\pi}_p = \{1, 2, \dots, p\} \setminus \{\hat{\pi}_1, \hat{\pi}_2, \dots, \hat{\pi}_{p-1}\}$;

Estimate the edge sets \hat{E} by assigning directions to the estimated undirected graph based on $\hat{\pi}$;

where $N_{\min} > 0$ is the minimum sample size in MRS algorithm.

The first condition is a stronger version of the identifiability assumption in Thm. 2.4 since we move from the population distribution to the finite sample setting. The second assumption is to control the tail behavior of the conditional distribution of each variable given its parents. It enables to control the accuracy of moments ratio scores (Eq. 4) even in high dimensional settings. The last assumption is also to control the accuracy of a moment ratio score by controlling the accuracy of method of moment estimators that are sensitive to sample sizes used.

We now state the second main result under Assumption 3.1. Since the true ordering π is possibly not unique, we use $\mathcal{E}(\pi)$ to denote the set of all the orderings that are consistent with the DAG G .

Theorem 3.2 (Recovery of the ordering). *Consider a GHD DAG model with the maximum degree of the graph is d . Suppose that the candidate parents set for all nodes are provided, and Assumptions 3.1(a)-(c) are satisfied. Then there exists constant $C_\epsilon > 0$ for $\epsilon > 0$ such that if sample size is sufficiently large $n > C_\epsilon \log^{2r+d}(\max(n, p)) \log(p)$, the MRS algorithm with r -th moments ratio scores recover the ordering with high probability.*

$$P(\hat{\pi} \in \mathcal{E}(\pi)) \geq 1 - \epsilon.$$

The detail of the proof is provided in Appendix. Intuitively, it makes sense because the method of moment estimator converges to the true moment as sample size n increases by weak law of large number. This allows the algorithm to recover a true ordering for the DAG G consistently.

Thm. 3.2 claims that if $n = \Omega(\log^{2r+d}(\max(n, p)) \log(p))$, our MRS algorithm accurately estimates the true ordering. Hence our MRS algorithm works in the high-dimensional ($p > n$) setting provided that the degree of the graph is bounded. This theoretical result is also consistent with learning Poisson DAG models shown in [11] where if $n = \Omega(\log^{5+d}(\max(n, p)))$ their algorithm recovers the ordering well. Since [11] uses the second order moments $r = 2$, both algorithms require asymptotically the same sample size. However we show that the MRS algorithm performs better the ODS algorithm through the simulation study because our algorithm uses the moments ratio instead of the moments difference that is proportional to magnitude of the moments.

Thm. 3.2 emphasizes that our algorithm exploits the sparsity of the graph and hence we can see the importance of Step 1) that enables the algorithm using the sparsity of the graph d . We provide simulation results to support that the MRS algorithm recovers a sparse graph in both low and high dimensional settings.

3.2 Computational Complexity

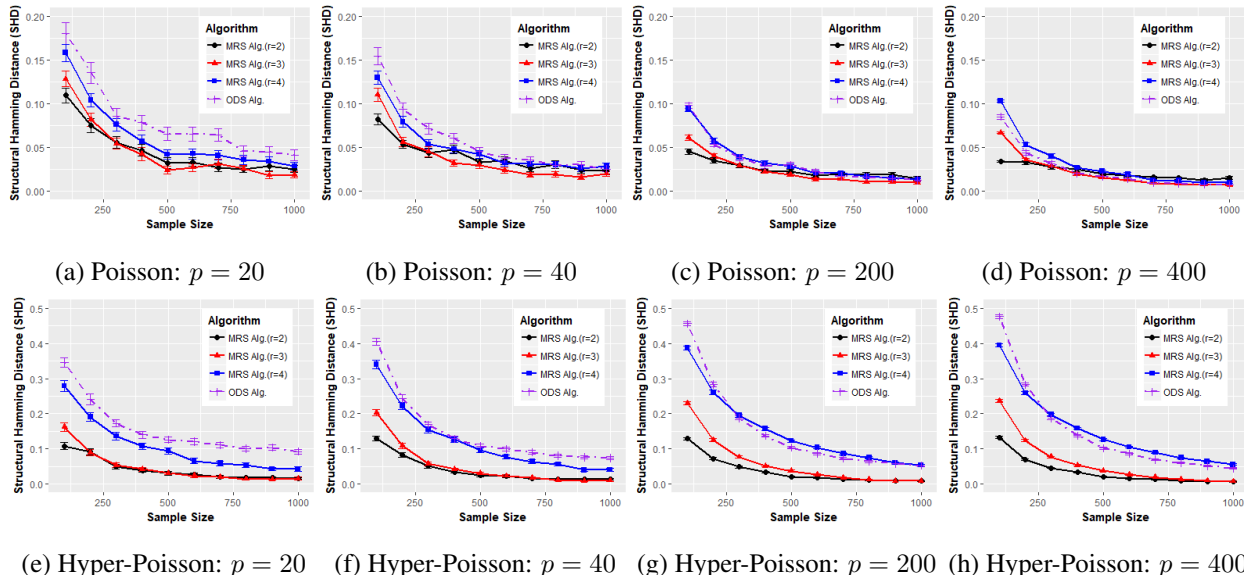
The MRS algorithm uses any existing algorithms with known computational complexity for Steps 1). Hence we focus on our novel Step 2) of the MRS algorithm. In Step 2), there are $(p-1)$ iterations and each iteration has a number of moment ratio scores to be computed which is bounded by $O(p)$. Hence the total number of scores to be calculated is $O(p^2)$. The computation time of each score is proportional to the sample size n , the complexity is $O(np^2)$. We verify this computational complexity through simulations in Section 4.

4 Simulation Experiments

In this section, we support our theoretical guarantees with synthetic data and show that our algorithm performs favorably compared to the ODS algorithm [11, 12] which learns Poisson DAG models. We evaluate algorithms in terms of how well the algorithm can recover the generative structure given finite datasets.

We conduct a simulation study using 100 realizations of p -node Poisson and Hyper-Poisson DAG models where the conditional distribution of each node given its parents is Hyper-Poisson with parameters $(b_j, \lambda_j(\text{Pa}(j)))_{j=1}^p$ where $\lambda_j(\text{Pa}(j)) = \exp(\sum_{k \in \text{Pa}(j)} \theta_{jk} X_k)$. The set of non-zero parameters $\theta_{jk} \in \mathbb{R}$ were generated uniformly at random in the range $\theta_{jk} \in [-2, -0.5]$. These values of parameter were chosen to ensure the count values do not blow up. We use the $b_j = 1$ for all j for Poisson DAG models and $b_j = 2$ for Hyper-Poisson DAG models. We considered more distributions and link functions, but for brevity, focus on these settings.

For all our simulation results, we generate DAG models with randomly generated directed graph structures while respecting the number of parents constraints for the DAG. We set the number of parents to two



(a) Poisson: $p = 20$ (b) Poisson: $p = 40$ (c) Poisson: $p = 200$ (d) Poisson: $p = 400$
(e) Hyper-Poisson: $p = 20$ (f) Hyper-Poisson: $p = 40$ (g) Hyper-Poisson: $p = 200$ (h) Hyper-Poisson: $p = 400$

Figure 2: Comparison of our algorithms using different values of $r = 2, 3, 4$ to ODS algorithm in terms of structural Hamming distance (SHD) for Poisson and Hyper-Poisson DAG models.

for sparse graphs. We also set the $r \in \{2, 3, 4\}$ and $N_{\min} = 5$ for computing the r -the moments ratio scores.

In order to authenticate the validation of Thm. 3.2, we measured the structural Hamming distance (SHD) of the true DAG and the estimated DAG given the true undirected edges. The SHD shows that how many directions of edges are incorrect that caused by a wrongly estimated ordering (see details in [17]). For the fair comparison to different graph size p , the normalized SHD is exploited by dividing it by the SHD of the true DAG and a DAG with a randomly generated ordering. We plot the normalized SHD as a function of sample size ($n \in \{100, 200, \dots, 1000\}$) for different node sizes ($p = \{20, 40, 200, 400\}$).

Fig. 2 provides a comparison of how accurately our MRS algorithm performs in terms of recovering ordering of the GHD DAG models. Fig. 2 supports our main theoretical results in Thm. 3.2: (i) GHD DAG models are identifiable; (ii) our algorithms recovers the ordering more accurately as sample size increases; (iii) our algorithm with $r = 4$ performs significantly worse than our algorithms with $r = 2, 3$ because because the required sample size for identifying the ordering is $n = \Omega(\log^{2r+d}(\max(n, p)) \log(p))$ that is highly depending on r ; and (iv) our algorithms recover the ordering even in high dimensional settings ($p = 400, n \leq 400$) in (d) and (f).

In Figure 3, we show the run-time of Step 2) of the MRS algorithm. We measured the run-time for learning Hyper-Poisson DAG models by varying (a) node size $p \in \{10, 20, \dots, 100\}$ with fixed sample size $n = 1000$ and (b) sample size $n \in \{100, 200, \dots, 1000\}$ with the fixed node size $p = 100$ and two parents of each node. As explained in Sec. 3.2, we can see that runtime of the algorithm is polynomial $O(np^2)$.

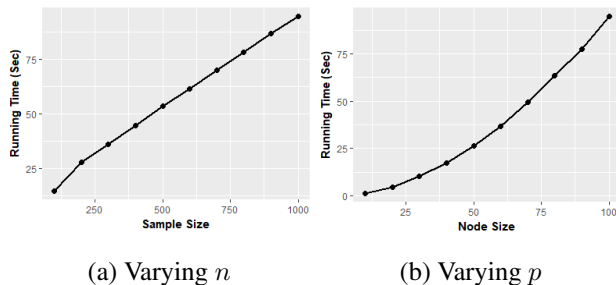


Figure 3: Running time of our algorithm for learning Hyper-Poisson with respect to (a) sample size $n \in \{100, 200, \dots, 1000\}$ with fixed $p = 100$, (b) node size $p \in \{10, 20, \dots, 100\}$ with fixed $n = 1000$.

5 Real Multi-variate Count Data: 2009/2010 NBA Player Statistics

We demonstrate the advantages of our graphical models for count-valued data by learning a 441 NBA player statistics from season 2009/2010 (see R package SportsAnalytics for detailed information) because we believe that some basketball statistics have causal or directional relationships. The original data set contains 24 covariates: player name, team name, players position, total minutes played, total number of field goals made, field goals attempted, threes made, threes attempted, free throws made, free throws attempted, offensive rebounds, rebounds, assists, steals, turnovers, blocks, personal fouls, disqualifications, technicals fouls, ejections, flagrant fouls, games started and total points. We eliminated player name, team name, number of games played, and players position, because our focus is to find the directional or causal relationships between statistics. We also eliminated ejections and flagrant fouls because both did not occur in our data set. Therefore the data set we consider contains 18 variables.

The original data set contains 24 covariates: player name, team name, players position, total minutes played, total number of field goals made, field goals attempted, threes made, threes attempted, free throws made, free throws attempted, offensive rebounds, rebounds, assists, steals, turnovers, blocks, personal fouls, disqualifications, technicals fouls, ejections, flagrant fouls, games started and total points. We eliminated player name, team name, number of games played, and players position, because our focus is to find the directional or causal relationships between statistics. We also eliminated ejections and flagrant fouls because both did not occur in our data set. Therefore the data set we consider contains 18 discrete variables.

Figure 4 (left) shows that the magnitude of NBA statistics are significantly different, and hence we expect our MRS algorithm would be more accurate than the comparison ODS algorithm. Moreover, Figure 4 (right) shows that all 18 variables are positively correlated. This makes sense because the total minutes played is likely to be positively correlated with other statistics, and some statistics have causal or directional relationships (e.g., the more shooting attempt implies the more shooting made).

We assumed each node conditional distribution given its parents is Hyper-Poisson because most of NBA statistics we consider are the number of successes or attempts counted in the season where each distribution of b_j is assumed as $\text{Var}(X_j)/\mathbb{E}(X_j)$ because we do not have any prior information of each distribution, but

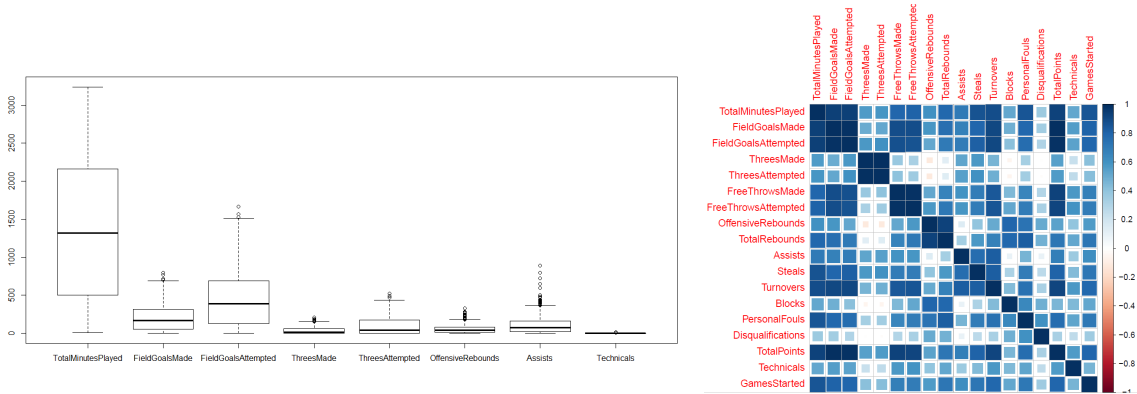


Figure 4: Box plots for some NBA statistics depending on positions (left). Box plots consider the total minutes played, total number of field goals made and attempted, threes made and attempted, offensive rebounds, assists, and technical fouls. Correlation Plots for NBA statistics (right). Blue represents a high correlation and white represents a small correlation.

this assumed b_j makes moment ratio scores near 1. Again the MRS and ODS algorithms are applied where GES algorithm is used in Step 1) because they are the only methods for fully identifying DAG models for multivariate count data. We note that GES algorithm provides a MEC, so we converted the estimated MEC to the skeleton for our algorithm.

Fig. 5 (a) shows the estimated graph using GES algorithm that does not provide any directions of edges. Figs. 5 (b) and (c) show the estimated directed graph using the MRS and ODS algorithms, respectively. We provide the differences between the estimated DAGs in Table. 2.

Explainable edges in Table. 2 shows the directed edges in the estimated DAG from the MRS algorithm while the estimated DAG from the ODS algorithm has opposite directions. This set of directed edges is more acceptable because the total minutes played would be a reason for other statistics, and a large number of shooting attempted would lead to the more shootings made. It is consistent to our simulation study that MRS algorithm provides more legitimate directed edges than the ODS algorithm when frequencies of variables are different. Unexplainable edges in Table. 2 shows the set of unaccountable edges in terms of causal or directional relationships regardless of directions. Hence they be introduced by Step 1) estimation of the skeleton.

In this paper, we provide the unique method that recovers a broader class of discrete DAG models possibly in high dimensional settings. However we acknowledge that our method also requires a strong known conditional distribution assumption and the proper choice of algorithm for Step 1).

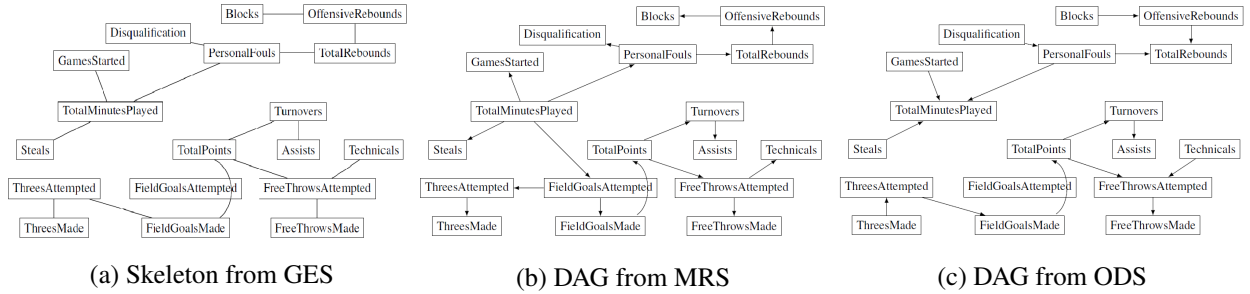


Figure 5: NBA players statistics undirected graph estimated by GES (left), DAG estimated by MRS (middle) and DAG estimated by ODS (right).

Explainable edges	TotalMinutesPlayed \rightarrow PersonalFouls and Steals ThreeAttempted \rightarrow ThreeMade, TotalRebounds \rightarrow OffensiveRebounds, PersonalFouls \rightarrow Disqualification, FieldGoalsAttempted \rightarrow FieldGoalsMade
Unexplainable edges	OffensiveRebounds \rightarrow Blocks, TotalPoins \rightarrow FreeThrowsAttempted FreeThrowsAttempted \rightarrow Techincals

Table 2: The set of directed edges in the estimated DAG from the MRS algorithm while the estimated DAG from the ODS does not contain in Figure 5.

References

- [1] David Maxwell Chickering. Optimal structure identification with greedy search. *The Journal of Machine Learning Research*, 3:507–554, 2003.
- [2] Michael F Dacey. A family of discrete probability distributions defined by the generalized hypergeometric series. *Sankhyā: The Indian Journal of Statistics, Series B*, pages 243–250, 1972.
- [3] Nir Friedman, Iftach Nachman, and Dana Peér. Learning bayesian network structure from massive datasets: the sparse candidate algorithm. In *Proceedings of the Fifteenth conference on Uncertainty in artificial intelligence*, pages 206–215. Morgan Kaufmann Publishers Inc., 1999.
- [4] Morten Frydenberg. The chain graph markov property. *Scandinavian Journal of Statistics*, pages 333–353, 1990.
- [5] David Heckerman, Dan Geiger, and David M Chickering. Learning Bayesian networks: The combination of knowledge and statistical data. *Machine learning*, 20(3):197–243, 1995.
- [6] Patrik O Hoyer, Dominik Janzing, Joris M Mooij, Jonas Peters, and Bernhard Schölkopf. Nonlinear causal discovery with additive noise models. In *Advances in neural information processing systems*, pages 689–696, 2009.
- [7] Adrienne W Kemp. A wide class of discrete distributions and the associated differential equations. *Sankhyā: The Indian Journal of Statistics, Series A*, pages 401–410, 1968.
- [8] Adrienne W Kemp and CD Kemp. A family of discrete distributions defined via their factorial moments. *Communications in Statistics-Theory and Methods*, 3(12):1187–1196, 1974.
- [9] Steffen L Lauritzen. *Graphical models*. Oxford University Press, 1996.
- [10] Joris Mooij, Dominik Janzing, Jonas Peters, and Bernhard Schölkopf. Regression by dependence minimization and its application to causal inference in additive noise models. In *Proceedings of the 26th annual international conference on machine learning*, pages 745–752. ACM, 2009.
- [11] Gunwoong Park and Garvesh Raskutti. Learning large-scale poisson dag models based on overdispersion scoring. In *Advances in Neural Information Processing Systems*, pages 631–639, 2015.
- [12] Gunwoong Park and Garvesh Raskutti. Learning quadratic variance function (qvf) dag models via overdispersion scoring (ods). *arXiv preprint arXiv:1704.08783*, 2017.
- [13] Jonas Peters and Peter Bühlmann. Identifiability of gaussian structural equation models with equal error variances. *Biometrika*, 101(1):219–228, 2014.

- [14] Jonas Peters, Joris Mooij, Dominik Janzing, and Bernhard Schölkopf. Identifiability of causal graphs using functional models. *arXiv preprint arXiv:1202.3757*, 2012.
- [15] Shohei Shimizu, Patrik O Hoyer, Aapo Hyvärinen, and Antti Kerminen. A linear non-Gaussian acyclic model for causal discovery. *The Journal of Machine Learning Research*, 7:2003–2030, 2006.
- [16] Peter Spirtes, Clark N Glymour, and Richard Scheines. *Causation, prediction, and search*. MIT press, 2000.
- [17] Ioannis Tsamardinos and Constantin F Aliferis. Towards principled feature selection: Relevancy, filters and wrappers. In *Proceedings of the ninth international workshop on Artificial Intelligence and Statistics*. Morgan Kaufmann Publishers: Key West, FL, USA, 2003.

6 Appendix

6.1 Proof for Prop1

Proof. For any integer r , [7] shows that

$$\mathbb{E}((X_j)_r | X_{\mathbf{Pa}(j)}) = \theta^r \prod_{i=1}^p \left(\frac{(a_i + r - 1)!}{(a_i - 1)!} \right) \prod_{j=1}^q \left(\frac{(b_j - 1)!}{(b_j + r - 1)!} \right). \quad (5)$$

Then, the expectation can be obtained when $r = 1$.

$$\mathbb{E}(X_j | X_{\mathbf{Pa}(j)}) = \theta \times \prod_{i=1}^p a_i \prod_{j=1}^q \frac{1}{b_j}.$$

By plugging this into Eqn. (3), we have

$$\mathbb{E}((X_j)_r | X_{\mathbf{Pa}(j)}) = \mathbb{E}(X_j | X_{\mathbf{Pa}(j)})^r \prod_{i=1}^p \left(\frac{(a_i + r - 1)!}{(a_i - 1)! a_i^r} \right) \prod_{j=1}^q \left(\frac{(b_j - 1)! b_j^r}{(b_j + r - 1)!} \right)$$

□

6.2 Proof for Thm1

Proof. Without loss of generality, we assume the true ordering is unique and $\pi = (\pi_1, \dots, \pi_p)$. For notational convenience, we define $X_{1:j} = (X_{\pi_1}, X_{\pi_2}, \dots, X_{\pi_j})$ and $X_{1:0} = \emptyset$. We prove identifiability of our CMR DAG models by mathematical induction.

For any node $j \in V \setminus \{\pi_1\}$, $\frac{\mathbb{E}((X_j)_r)}{f_j(\mathbb{E}(X_j))} > 1$ from the identifiability assumption 2.3 while

$$\frac{\mathbb{E}((X_{\pi_1})_r)}{f_{\pi_1}(\mathbb{E}(X_{\pi_1}))} = \frac{f_{\pi_1}(\mathbb{E}(X_{\pi_1}))}{f_{\pi_1}(\mathbb{E}(X_{\pi_1}))} = 1$$

by the definition of CMR DAG models. Hence we can determine π_1^* as the first element of the causal ordering.

For the $(m - 1)^{th}$ element of the ordering, assume that the first $m - 1$ elements of the ordering and their parents are correctly estimated. Now, we consider the m^{th} element of the causal ordering and its parents. By Assumption 2.3, for $j \in \{m, m + 1, \dots, p\}$, $\frac{\mathbb{E}(X_j | X_{1:(m-1)})}{f_j(\mathbb{E}((X_j)_r | X_{1:(m-1)}))} > 1$. In addition, it is clear that $\frac{\mathbb{E}((X_{\pi_m})_r | X_{1:(m-1)})}{f_{\pi_m}(\mathbb{E}(X_{\pi_m} | X_{1:(m-1)}))} = \frac{\mathbb{E}((X_{\pi_m})_r | X_{\mathbf{Pa}(\pi_m)})}{f_{\pi_m}(\mathbb{E}(X_{\pi_m} | X_{\mathbf{Pa}(\pi_m)}))} = 1$. Hence we can estimate a valid m^{th} component of the causal ordering π_m and its parents by testing whether the r-th moments ratio is whether greater than or equal to 1. By induction this completes the proof. □

6.3 Proof for Thm2

Proof. We first reintroduce some necessary notations and definitions to make the proof concise. Without loss of generality, assume that the true ordering is unique and $\pi = (\pi_1, \dots, \pi_p)$. In addition for ease of notation, we drop the r in the r -th moments ratio scores and

$$\mathcal{S}(j, S) := \frac{\mathbb{E}((X_j)_r | X_S)}{f_j(\mathbb{E}(X_j | X_S))} \quad \text{and} \quad \widehat{\mathcal{S}}(j, S) := \frac{\widehat{\mathbb{E}}((X_j)_r | X_S)}{f_j(\widehat{\mathbb{E}}(X_j | X_S))}.$$

We define the following events:

For each node $j \in V$ and set $S \subset V \setminus (\text{De}(j) \cup \{j\})$ and $\epsilon > 0$,

$$\begin{aligned} \zeta_1 &:= \left\{ \min_{j=1, \dots, p-1} \min_{k=j+1, \dots, p} \left| \mathcal{S}(j, \pi_k) - \widehat{\mathcal{S}}(j, \pi_k) \right| > \frac{M_{\min}}{2} \right\} \\ \zeta_2 &:= \left\{ \max_{j \in V} \left| \widehat{\mathbb{E}}(X_j^r | X_S) - \mathbb{E}(X_j^r | X_S) \right| < \epsilon \right\} \\ \zeta_3 &:= \left\{ \max_{j \in V} \left| f_j \left(\widehat{\mathbb{E}}(X_j | X_S) \right) - f_j \left(\mathbb{E}(X_j | X_S) \right) \right| < \frac{\epsilon}{2} \right\} \\ \zeta_4 &:= \left\{ \max_{j \in V} \left| \left(\sum_{k=0}^{r-1} s(r, k) \widehat{\mathbb{E}}(X_j^k | X_S) - \sum_{k=0}^{r-1} s(r, k) \mathbb{E}(X_j^k | X_S) \right) \right| < \frac{\epsilon}{2} \right\} \\ \zeta_5 &:= \left\{ \max_{j \in V} \max_{i \in \{1, 2, \dots, n\}} |X_j^{(i)}| < 4 \log \eta \right\} \end{aligned} \quad (6)$$

Here we use method of moments estimators $\frac{1}{n} \sum_{i=1}^n (X_j^{(i)})^k$ as unbiased estimators for $\mathbb{E}(X_j^k)$ for all $1 \leq k \leq r$.

We prove our algorithm recover the ordering of the CMR DAG model in the high dimensional settings. The probability that ordering is correctly estimated from our method can be written as

$$\begin{aligned} &P(\widehat{\pi} = \pi) \\ &= P\left(\widehat{\mathcal{S}}(1, \pi_1) < \min_{j=2, \dots, p} \widehat{\mathcal{S}}(1, \pi_j), \widehat{\mathcal{S}}(2, \pi_2) < \min_{j=3, \dots, p} \widehat{\mathcal{S}}(1, \pi_j), \dots, \widehat{\mathcal{S}}(p-1, \pi_{p-1}) < \widehat{\mathcal{S}}(p-1, \pi_p)\right) \\ &= P\left(\min_{j=1, \dots, p-1} \min_{k=j+1, \dots, p} \widehat{\mathcal{S}}(j, \pi_k) - \widehat{\mathcal{S}}(j, \pi_j) > 0\right) \\ &= P\left(\min_{j=1, \dots, p-1} \min_{k=j+1, \dots, p} \left\{ (\mathcal{S}(j, \pi_k) - \mathcal{S}(j, \pi_j)) - (\mathcal{S}(j, \pi_k) - \widehat{\mathcal{S}}(j, \pi_k)) + (\mathcal{S}(j, \pi_j) + \widehat{\mathcal{S}}(j, \pi_j)) \right\} > 0\right) \\ &\geq P\left(\min_{j=1, \dots, p-1} \min_{k=j+1, \dots, p} \{(\mathcal{S}(j, \pi_k) - \mathcal{S}(j, \pi_j))\} > M_{\min}, \text{ and} \right. \\ &\quad \left. \min_{j=1, \dots, p-1} \min_{k=j+1, \dots, p} \left| \mathcal{S}(j, \pi_k) - \widehat{\mathcal{S}}(j, \pi_k) \right| < \frac{M_{\min}}{2} \right) \end{aligned}$$

By Assumption 3.1 (A1) $\mathbb{E}((X_j)_r | X_S) - f_j(\mathbb{E}(X_j | X_S)) > M_{\min}$, the above lower bound of the

probability that ordering is correctly estimated using our method is reduced to

$$\begin{aligned}
P(\widehat{\pi} = \pi) &\geq 1 - P\left(\min_{j=1, \dots, p-1} \min_{k=j, \dots, p} \left| \mathcal{S}(j, \pi_k) - \widehat{S}(j, \pi_k) \right| > \frac{M_{\min}}{2}\right) \\
&= 1 - P(\zeta_1) \\
&= 1 - \{P(\zeta_1 \mid \zeta_2, \zeta_3, \zeta_4)P(\zeta_2, \zeta_3, \zeta_4) + P(\zeta_1 \mid (\zeta_2, \zeta_3, \zeta_4)^c)P((\zeta_2, \zeta_3, \zeta_4)^c)\} \\
&\geq 1 - \{P(\zeta_1 \mid \zeta_2, \zeta_3, \zeta_4) + P((\zeta_2, \zeta_3, \zeta_4)^c)\} \\
&= 1 - \{P(\zeta_1 \mid \zeta_2, \zeta_3, \zeta_4) + P((\zeta_2, \zeta_3, \zeta_4)^c \mid \zeta_5)P(\zeta_5) + P((\zeta_2, \zeta_3, \zeta_4)^c \mid \zeta_5^c)P(\zeta_5^c)\} \\
&\geq 1 - \{P(\zeta_1 \mid \zeta_2, \zeta_3, \zeta_4) + P((\zeta_2, \zeta_3, \zeta_4)^c \mid \zeta_5) + P(\zeta_5^c)\} \\
&\geq 1 - \left\{ \underbrace{P(\zeta_1 \mid \zeta_2, \zeta_3, \zeta_4)}_{\text{Prop6.1}} + \underbrace{P(\zeta_2^c \mid \zeta_5) + P(\zeta_3^c \mid \zeta_5) + P(\zeta_4^c \mid \zeta_5)}_{\text{Prop6.2}} + \underbrace{P(\zeta_5^c)}_{\text{Prop6.3}} \right\}.
\end{aligned}$$

Next we introduce the following three propositions to show that the above lower bound converges to 1. The first proposition proves that estimated score is accurate under some regularity conditions.

Proposition 6.1. *Given the sets $\zeta_2, \zeta_3, \zeta_4$ in (6), $P(\zeta_1 \mid \zeta_2, \zeta_3, \zeta_4) = 0$ if one of the following conditions are satisfied*

(i) $2|\mathbb{E}((X_j)_r \mid x)| + (2 - M_{\min})|f_j(\mathbb{E}(X_j \mid x))| < 0$, or

(ii) $\epsilon < \frac{M_{\min} f_j(\mathbb{E}(X_j \mid x))^2}{(2|\mathbb{E}((X_j)_r \mid x)| + (2 - M_{\min})|f_j(\mathbb{E}(X_j \mid x))|)}$.

The first condition (i) is satisfied if M_{\min} in the identifiability assumption 2.3 is sufficiently large and the second condition (ii) is satisfied if ϵ is sufficiently small. This means that the r -th factorial moment estimator is sufficiently accurate.

The second propositions show the consistent estimators for higher order moment is X_j^k for $1 \leq k \leq r$ given the set ζ_5 .

Proposition 6.2. *For any set $S \subset V \setminus (De(j) \cup \{j\})$ and $\epsilon > 0$,*

(i) For ζ_2 ,

$$P(\zeta_2^c \mid \zeta_5) \leq 2p \exp \left\{ -\frac{2N_{\min} \epsilon^2}{(4 \log^2 \eta)^r} \right\}.$$

(ii) For ζ_3 ,

$$P(\zeta_3^c \mid \zeta_5) \leq 2p \exp \left\{ -\frac{N_{\min} \epsilon^2}{8(f'_j(m))^2 \log^2 \eta} \right\}.$$

(iii) For ζ_4 ,

$$P(\zeta_4^c \mid \zeta_5) \leq 2p \exp \left\{ -\frac{2N_{\min} \epsilon^2}{\max_{k \in \{1, \dots, r-1\}} s(r, k) (4 \log^2 \eta)^r} \right\}.$$

where N_{\min} is a predetermined minimum sample size from Assumption 3.1 (A3) and $s(r, k)$ is Stirling numbers of the first kind.

Proposition 6.3. *Under the assumption 3.1 (A2),*

$$P(\zeta_5^c) \leq \frac{V_1}{\eta^2}.$$

Hence our method recovers the true ordering at least of

$$\begin{aligned} P(\hat{\pi} = \pi) &\geq 1 - \left\{ \underbrace{P(\zeta_1 | \zeta_2, \zeta_3)}_{\text{Prop6.1}} + \underbrace{P(\zeta_2^c | \zeta_5) + P(\zeta_3^c | \zeta_5)}_{\text{Prop6.2}} + \underbrace{P(\zeta_5^c)}_{\text{Prop6.3}} \right\} \\ &= 1 - 2p.\text{exp} \left\{ -\frac{2N_{\min}\epsilon^2}{(4\log^2\eta)^r} \right\} - 2p.\text{exp} \left\{ -\frac{N_{\min}\epsilon^2}{8(f'_j(m))^2 \log^2\eta} \right\} \\ &\quad - 2p.r.\text{exp} \left\{ -\frac{2N_{\min}\epsilon^2}{\max_{k \in \{1, \dots, r-1\}} s(r, k)(4\log^2\eta)^r} \right\} - \frac{V_1}{\eta^2} \end{aligned}$$

This result claims that if $N_{\min} = O(\log^{2r}(\eta) \log(p))$, our algorithm correctly estimate the ordering of the graph.

Finally, we show the relationship between the sample size n and N_{\min} . Suppose that d is the maximum number of parents of a node. Then the maximum size of the candidate parents set is d . The scenario is that a conditioning set has two possible cases. If there is only one element for the conditioning set, there is no difference between the conditional and marginal distributions. In the best case, $n = 2N_{\min}$ when there are two conditional distributions $|\mathcal{X}_C| = 2$. Hence if $n = O((\log^{2r}(\eta)(\log(p) + \log(r)))$, our algorithm works in the high dimensional settings. In the worst case given ζ_5 , the sample size is $n = (4\log(\eta)^d - 2)(N_{\min} - 1) + 2N_{\min} = 4\log(\eta)^d(N_{\min} - 1) + 2$ where the number of all elements of $\{x \in \mathcal{X}_C \mid \sum_i^n \mathbf{1}(X_C^{(i)} = x) \geq N_{\min}\}$ is two and all other elements of \mathcal{X}_C has $N_{\min} - 1$ repetitions. In this worst case, if $n = O(\log(\eta)^{(2r+d)}(\log(p) + \log(r)))$ our algorithm correctly recover the ordering with high probability. □

6.3.1 Proof for Proposition 6.1

Proof. For ease of notation, let $\eta = \max\{n, p\}$ and $\hat{\mathcal{S}}_r(m, j)(x) := \frac{\hat{\mathbb{E}}((X_j)_r | X_{\hat{C}_{mj}} = x)}{f_j(\hat{\mathbb{E}}(X_j | X_{\hat{C}_{mj}} = x))}$ for $x \in \mathcal{X}_{\hat{C}_{mj}}$. Then, the moments ratio score is

$$\hat{\mathcal{S}}_r(m, j) := \sum_{x \in \mathcal{X}_{\hat{C}_{mj}}} \frac{n(x)}{n_{\hat{C}_{mj}}} \hat{\mathcal{S}}_r(m, j)(x). \quad (7)$$

For any $j \in V$, $k \in \{j, \dots, p\}$ and $x \in \mathcal{X}_{\widehat{C}_{m_j}}$, we have

$$\begin{aligned}
& P \left(\left| \widehat{S}(j, k)(x) - \mathcal{S}(j, k)(x) \right| > \frac{M_{\min}}{2} \mid \zeta_2, \zeta_3 \right) \\
&= P \left(\left| \frac{\widehat{\mathbb{E}}((X_j)_r \mid x)}{f_j(\widehat{\mathbb{E}}(X_j \mid x))} - \frac{\mathbb{E}((X_j)_r \mid x)}{f_j(\mathbb{E}(X_j \mid x))} \right| > \frac{M_{\min}}{2} \mid \zeta_2, \zeta_3 \right) \\
&\leq P \left(\frac{\mathbb{E}((X_j)_r \mid x) + \epsilon}{f_j(\mathbb{E}(X_j \mid x)) - \epsilon} - \frac{\mathbb{E}((X_j)_r \mid x)}{f_j(\mathbb{E}(X_j \mid x))} > \frac{M_{\min}}{2} \text{ or } \frac{\mathbb{E}((X_j)_r \mid x)}{f_j(\mathbb{E}(X_j \mid x))} - \frac{\mathbb{E}((X_j)_r \mid x) - \epsilon}{f_j(\mathbb{E}(X_j \mid x)) + \epsilon} > \frac{M_{\min}}{2} \right) \\
&= P \left(\frac{\epsilon(f_j(\mathbb{E}(X_j \mid x)) + \mathbb{E}((X_j)_r \mid x))}{f_j(\mathbb{E}(X_j \mid x))(f_j(\mathbb{E}(X_j \mid x)) + \epsilon)} > \frac{M_{\min}}{2} \text{ or } \frac{\epsilon(f_j(\mathbb{E}(X_j \mid x)) + \mathbb{E}((X_j)_r \mid x))}{f_j(\mathbb{E}(X_j \mid x))(f_j(\mathbb{E}(X_j \mid x)) - \epsilon)} > \frac{M_{\min}}{2} \right) \\
&\leq P \left(\frac{\epsilon(|f_j(\mathbb{E}(X_j \mid x))| + |\mathbb{E}((X_j)_r \mid x)|)}{|f_j(\mathbb{E}(X_j \mid x))|(f_j(\mathbb{E}(X_j \mid x)) + \epsilon)} > \frac{M_{\min}}{2} \text{ or } \frac{\epsilon(|f_j(\mathbb{E}(X_j \mid x))| + |\mathbb{E}((X_j)_r \mid x)|)}{|f_j(\mathbb{E}(X_j \mid x))|(f_j(\mathbb{E}(X_j \mid x)) - \epsilon)} > \frac{M_{\min}}{2} \right) \\
&= P \left(M_{\min} f_j(\mathbb{E}(X_j \mid x))^2 < \epsilon(2|\mathbb{E}((X_j)_r \mid x)| + (2 - M_{\min})|f_j(\mathbb{E}(X_j \mid x))|) \right).
\end{aligned}$$

Some simple calculations yield that the above upper bound is zero if either

- (i) $2|\mathbb{E}((X_j)_r \mid x)| + (2 - M_{\min})|f_j(\mathbb{E}(X_j \mid x))| < 0$ or
- (ii) $\epsilon < \frac{M_{\min} f_j(\mathbb{E}(X_j \mid x))^2}{(2|\mathbb{E}((X_j)_r \mid x)| + (2 - M_{\min})|f_j(\mathbb{E}(X_j \mid x))|)}$.

□

6.3.2 Proof for Proposition 6.2

Since the proof for Proposition 6.2 (i) - (iii) are analogous, we provide the proof for (iii) and then we provide the proof for (ii).

Proof. Using Hoeffding's inequality given ζ_5 , for $1 \leq k \leq r$ and any $\epsilon > 0$,

$$P \left(\left| \widehat{\mathbb{E}}(X_j^k \mid X_S) - \mathbb{E}(X_j^k \mid X_S) \right| > \epsilon \right) \leq 2p \cdot \exp \left\{ -\frac{N_{\min} \epsilon^2}{8 \log^{2k} \eta} \right\}. \quad (8)$$

Hence, given ζ_5 ,

$$\begin{aligned}
& P \left(\left| \sum_{k=0}^{r-1} s(r, k) \widehat{\mathbb{E}}(X_j^k \mid X_S) - \sum_{k=0}^{r-1} s(r, k) \mathbb{E}(X_j^k \mid X_S) \right| > \epsilon \mid \zeta_5 \right) \\
&\leq \sum_{k=1}^{r-1} P \left(\left| \widehat{\mathbb{E}}(X_j^k \mid X_S) - \mathbb{E}(X_j^k \mid X_S) \right| > \frac{\epsilon}{s(r, k)} \mid \zeta_5 \right) \\
&\leq \sum_{k=1}^{r-1} 2p \cdot \exp \left\{ -\frac{N_{\min} \epsilon^2}{8 s(r, k) \log^{2k} \eta} \right\} \\
&\leq 2rp \cdot \exp \left\{ -\frac{N_{\min} \epsilon^2}{8 \max_k s(r, k) \log^{2r} \eta} \right\}.
\end{aligned}$$

□

Now we provide the proof for (ii).

Proof. By Mean value theorem, we obtain

$$f_j(\widehat{\mathbb{E}}(X_j | X_S)) - f_j(\mathbb{E}(X_j | X_S)) = f'_j(m) \left(\widehat{\mathbb{E}}(X_j | X_S) - \mathbb{E}(X_j | X_S) \right). \quad (9)$$

where m is some point between $\widehat{\mathbb{E}}(X_j)$ and $\mathbb{E}(X_j)$.

Using Hoeffding's inequality given ζ_5 , for any $\epsilon > 0$,

$$\begin{aligned} P \left(\min_{j \in V} f_j \left(\widehat{\mathbb{E}}(X_j | X_S) \right) - f_j(\mathbb{E}(X_j)) > \epsilon \mid \zeta_5 \right) &\leq p \min_{j \in V} P \left(\left(\widehat{\mathbb{E}}(X_j | X_S) - \mathbb{E}(X_j | X_S) \right) > \frac{\epsilon}{f'_j(m)} \mid \zeta_5 \right) \\ &\leq 2p \cdot \exp \left\{ -\frac{N_{\min} \epsilon^2}{8(f'_j(m))^2 \log^2 \eta} \right\}. \end{aligned}$$

□

6.3.3 Proof for Proposition 6.3

Proof.

$$\begin{aligned} P(\zeta_5^c) &= P \left(\min_{j \in V} \min_{i \in \{1, 2, \dots, n\}} P \left| (X_j^{(i)})_r \right| > 4 \log \eta \right) \\ &\leq np P \left(P \left| (X_j^{(i)})_r \right| > 4 \log \eta \right) \\ &\leq np \frac{\mathbb{E}(\exp(X_j^{(I)}))}{\eta^4} \\ &\leq np \frac{\mathbb{E}(\mathbb{E}(\exp(X_j^{(i)}) \mid X_{\text{Pa}(j)}))}{\eta^4} \\ &\stackrel{(a)}{\leq} np \frac{V_1}{\eta^4} \\ &\leq \frac{V_1}{\eta^2}. \end{aligned}$$

Inequality (a) is from Assumption 3.1 (A2).

□